ADVANCED MATERIALS
www.advmat.de

A Stable Polyaniline-Benzoquinone-Hydroquinone Supercapacitor

David Vonlanthen, Pavel Lazarev, Kimberly A. See, Fred Wudl, and Alan J. Heeger**

Supercapacitors (electrochemical capacitors) are energy storage devices that exhibit high power density discharging hundreds of times faster than batteries, as required for power and backup applications in vehicles, consumer electronics and solar cells.[1] Commercially available supercapacitors use carbon electrodes which display low capacitance as the energy is stored by the double-layer mechanism.[2] Alternatively, redox-active materials (pseudo-capacitive materials) use faradaic processes to achieve higher specific capacities (C_s). Materials under research include redox-active polymer electrodes and carbon electrodes functionalized with polymers, transition metals and small molecules.[3,5b] In addition, a poly-pyrrole/lignin composite was used to increase the pseudo-capacitance of polymer electrodes.[4] Indeed, quinone-functionality is gaining attention for its ability to store 2 e^-/2 H^+ per quinone[3a,4] unit and its ability to enhance capacities in double-layer supercapacitors.[3a,5b,5d]

Among all pseudo-capacitive[3b] materials for supercapacitors, polyaniline is one of the best candidates due to its high faradaic activity,[3c,6] good electrical conductivity[7] and high surface area that can be achieved by tailor-made synthetic routes.[8] Moreover, polyaniline is an abundant, low-cost, and easily processable material, which makes it useful in energy storage devices.[1c,9] However, poor cycling stability of electro-active polymers hampers the development of polymer-based supercapacitor and battery devices.[1a,3b,10] Supercapacitors require a long cycle life-time[11] (>10,000 cycles) which is not often achieved with polymers, although improved stabilities were demonstrated in ultrafine dispersions of polyaniline on high-surface area carbon substrates.[5a]

Herein, we demonstrate that the previously unreported combination of conventional porous polyaniline and quinone electrolytes gives supercapacitors with unmatched cycling stability (>50,000) and high specific capacitance. We combine two redox systems: polyaniline as the porous electrochemically-active material and the benzoquinone-hydroquinone (BQHQ) redox couple as an electrolyte. Introduction of a second redox-system into the supercapacitor creates a tunable redox shuttle that controls electron transfer processes at the polyaniline-modified electrodes. Quinones are particularly excellent redox-active electrolytes (acting as mediating agents) due to their small size (high mobility) and the excellent electrochemical reversibility at low pH which makes them compatible with the family of acid-doped polymers.[7,12]

The supercapacitor devices (**Figure 1**a) were fabricated by casting defined quantities of conventional polyaniline emeraldine-base (P) doped with H_2SO_4 onto platinum (Pt) current collectors. UV-VIS-NIR spectroscopy confirmed the presence of the metallic emeraldine-salt form of polyaniline (EM) after the drop-casting process (Figure S4). The BET surface area is 22.1 $m^2\ g^{-1}$ for the emeraldine-di-hydrogensulfate (36.6 $m^2\ g^{-1}$ for the emeraldine-base, Figure S5). Analysis with scanning electron microscopy (SEM) of the emeraldine salt film revealed a network of interpenetrating particles creating a porous electrode structure after drop-casting (Figure S6). Two identical polymer-modified electrodes were sandwiched and separated by an ion-and-molecule-permeable glass membrane soaked with the quinone mediators (BQ and HQ) and the supporting electrolyte (H_2SO_4/AcOH). The addition of acetic acid was essential to keep both BQ and HQ freely disassociated in the electrolytic system, preventing the formation of the BQHQ acceptor-donor complex (quinhydrone).[13]

To evaluate the long-term cycling performance of the polymer-supercapacitors, galvanostatic charge-discharge experiments were performed. The galvanostatic discharge method is the most accepted measurement method for determining capacities of supercapacitors.[14]

The addition of BQHQ redox-electrolytes greatly enhanced the cycling stability of the supercapacitors with polymeric electrodes (P-BQHQ). The advantage of the presented multi-redox approach over the conventional polymer supercapacitors (P) is evident from cycling experiments (Figure 1b and 1c). The supercapacitor (P) with H_2SO_4/AcOH electrolyte and no added BQHQ shows an initial a specific capacitance (C_s) of 418 F/g followed by a rapid loss typical of polymer electrodes of 10% capacitance after 350 cycles and a capacitance retention of 80% (334 F/g) after 2800 cycles (Figure 1b, grey curve). In the supercapacitor with BQHQ-electrolytes (P-BQHQ), the capacitance starts at 86% of the maximum capacitance, reaches 95% after 7 cycles and 100% of the maximal capacitance (524 F/g) after 200 cycles (Figure 1b, black curve). This feature indicates the presence of a complex equilibration/intercalation process at the polymer-modified electrodes involving both the reductive hydroquinone and the oxidative benzoquinone molecules. The long-term cycling behavior displayed in **Figure 2**c illustrates outstanding performance over 50,000 cycles. After the first 13,000 cycles (Figure 2c, upper graph), capacitance retention of

Dr. D. Vonlanthen, Prof. F. Wudl, Prof. A. J. Heeger
Center for Polymers and Organic Solids
University of California
Santa Barbara, Santa Barbara, California 93106-5090, USA
E-mail: david.vonlanthen@gmail.com;
ajhe1@physics.ucsb.edu
K. A. See
Department of Chemistry & Biochemistry
University of California
Santa Barbara, Santa Barbara, California 93106-5090, USA
Dr. P. Lazarev
Cryscade Inc
2225 East Bayshore Rd. #200, Palo Alto, CA 94303, USA

DOI: 10.1002/adma.201400966

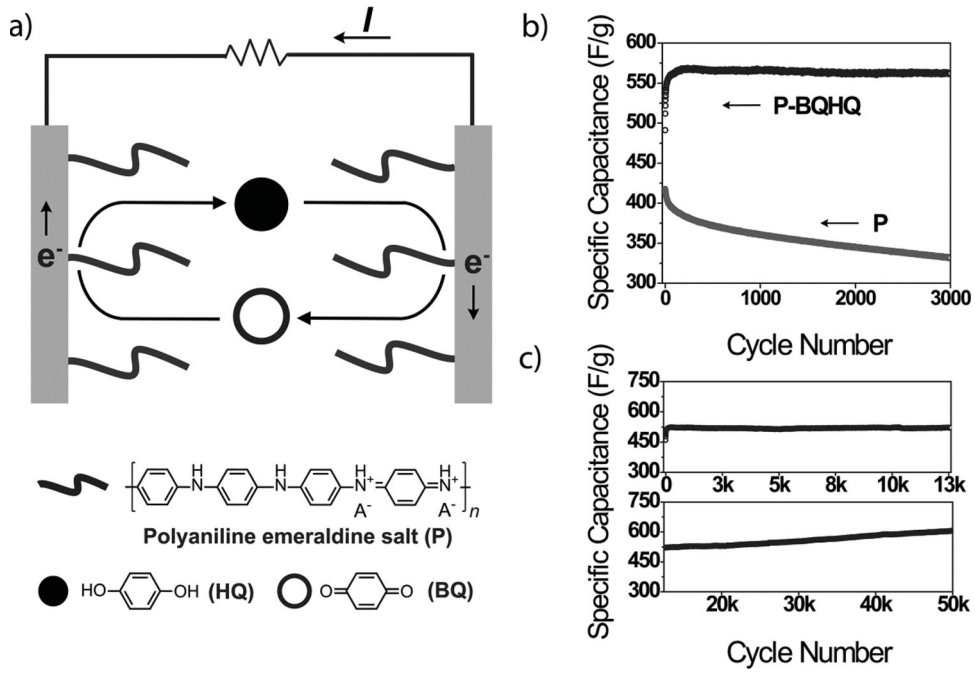

Figure 1. a) Supercapacitor with two identical polymer-modified electrodes prepared by depositing polyaniline in the metallic emeraldine-salt form (A^- = hydrogensulfate anions) onto Pt-metal current collectors. The electrodes are separated by an ion-and-molecule-permeable membrane and soaked with the quinone and supporting electrolytes (H_2SO_4/AcOH). During charge and discharge operations BQ and HQ electrolytes undergo redox processes at the electrodes. b) The specific capacity of the supercapacitors versus the number of cycles obtained from galvanostatic charge–discharge experiments (12.5 mA/cm^2) in BQHQ/H_2SO_4/AcOH (P-BQHQ, black curve) and in H_2SO_4/AcOH electrolyte solution (P, grey curve). c) Cycling behavior of the P-BQHQ supercapacitor over a longer time scale (50,000 cycles).

99.5% was observed. At longer times (Figure 2c, lower graph) a further increase of the capacitance of 15% was measured, demonstrating the persistent stability of the polymeric electrodes in the presence of the BQHQ quinoid electrolytes. This increase in capacitance may be due to adsorption of the quinones at the electrodes or due to a change in the ratio of the BQ/HQ mediators near the electrodes during the repetitive cycling. These observed long-term stability characteristics are in sharp contrast to conventional polymer devices and exceed those of polymer-carbon hybrid-supercapacitors[5a,9a,9c,9d] and quinone-based supercapacitors with carbon electrodes.[3a]

The performance, turn-on characteristics, and long-term stability were found to be dependent on the detailed mixture of benzoquinone and hydroquinone used.

In order to understand the stability, the electrochemical behavior of single components at controlled potentials was analyzed using a 3-electrode setup. Figure 2a shows the cyclic voltammograms (CV) of all compounds used in the supercapacitors. The sweep rate was 25 mV/s for all CVs and scanning was from –0.1 V in the positive direction. Polyaniline exhibits two characteristic redox processes[6,20]: the anodic wave at 0.26 V and the cathodic wave at –0.01 V corresponding to the transitions between leucoemeraldine (LE) and the metallic emeraldine (EM). A shifted "first cycle" anodic wave was not observed during the CV measurement that would indicate the presence of leucoemeraldine. This further confirmed the presence of the emeraldine-salt. The anodic wave at 0.85 V and the cathodic wave at 0.75 V correspond to the transitions between EM and the unstable pernigraniline (PE).[15] The cathodic reduction wave of BQ→HQ is at 0.21 V and overlaps well with the electrochemical potential of the EM-LE transition. The anodic oxidation wave of HQ→BQ is located at 0.63 V which is at a less-positive potential than the unfavorable EM-PE transition.[15]

We speculate that the unstable PE state remains unpopulated during charge–discharge cycles because of electron-transfer between polyaniline and the quinones. This results in the inherent cycling stability displayed in Figures 1c and 2c. Moreover, the overall faradaic activity of the polymer, including ion-insertion and expulsion processes,[3b,16] is lowered which further enhances the stability of the polymer.

To confirm the proposed mechanism for the enhanced stability, the cycling behavior of the P-BQHQ supercapacitor was compared with the P-HQ device (Figure 2b, black curve) where solely electron-donating HQ electrolytes are employed. Additionally, the cycling behavior of the P-BQ supercapacitor is analyzed where solely electron-accepting BQ electrolytes are used (Figure 2b, grey curve). A rapid decrease of the capacitance was observed in the P-HQ device. After an initial high C_s of 817 F/g, a loss of 30% of the charge capacitance after a few cycles (11) was noted which continuously decreased to a capacitance of 426 F/g (capacity retention of 52%), much lower than the capacitance of the P-BQHQ device. However, after the initial C_s drop of 52% the P-HQ devices remain stable up to 50,000 cycles (Figure 1c). In contrast, the capacitance of the tested P-BQ supercapacitors dropped rapidly. After an initial high capacitance (629 F/g), a loss of 50% of C_s was observed after only 400 cycles and a loss of 80% of C_s was observed after 1600

Adv. Mater. 2014,
DOI: 10.1002/adma.201400966

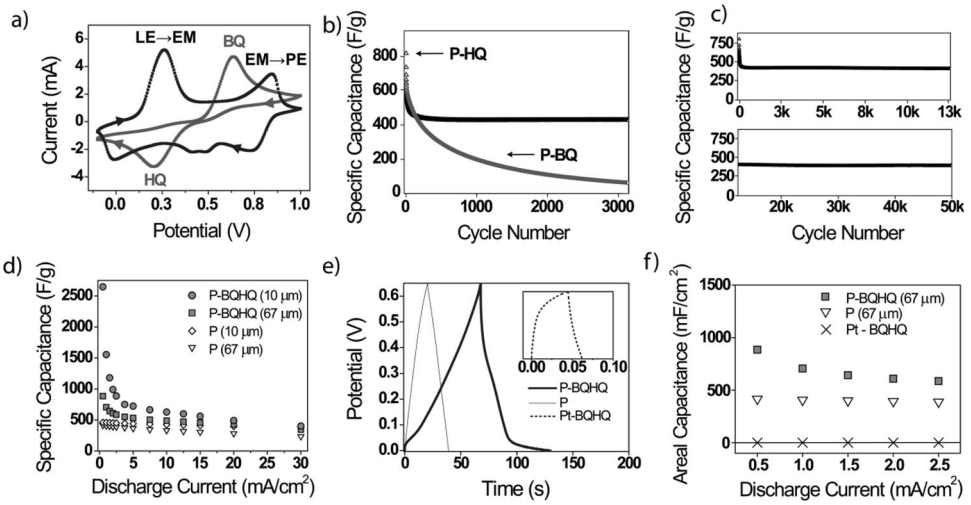

Figure 2. a) Cyclic voltammetry (3-electrode setup) of a single polyaniline-modified electrode (10 µm, black voltammogram) measured against a Pt wire (CE) with Ag/AgCl (RE) in supporting electrolytes (H_2SO_4, 1 M/AcOH 30%). The scan rate is 25 mV/s. Two transitions, LE-EM and EM-PE are observed. CV of the BQHQ solution (73 mM, 1:1) is measured with a bare platinum electrode (WE, 1 cm^2), against a Pt wire (CE) with Ag/AgCl (RE) at a scan rate of 25 mV/s (grey voltammogram). The CV shows a cathodic reduction wave (BQ to HQ) at 0.21 V and an anodic oxidation wave (HQ to BQ) at 0.63 V. b) The C_s of the supercapacitors with the number of cycles obtained from galvanostatic charge–discharge experiments (12.5 mA/cm^2) employing HQ (P-HQ, black curve) and BQ (P-BQ, grey curve) as redox-active electrolytes. c) Cycling performance of the P-HQ supercapacitor over longer time scales. d) Interdependence of discharge-rate and C_s values from galvanostatic discharge of the P and P-BQHQ supercapacitors. e) Single galvanostatic charge-discharge curves at 1 mA/cm^2 of the P, P-BQHQ and Pt-BQHQ (inset) supercapacitors. f) Areal capacitance for the P, P-BQHQ and Pt-BQHQ supercapacitors. Negligible capacitance is measured for the Pt-BQHQ system (X). HQBQ-Polyaniline devices (■) show enhanced capacitance compared to polyaniline devices (▽) due to a cooperative effect of the porous polymer film and the quinones. In all measurements H_2SO_4 (1 M) with AcOH (30%) was used as the supporting electrolyte.

cycles. This drop in performance is faster than in the conventional polymer-device P (Figure 1b, grey curve).

AC-impedance measurements further support these findings. The equivalent series resistance (ESR) estimated from the high frequencies (~4.5 Ω) as well as the charge transfer resistance extracted from the small semicircles in the Nyquist plots (Figure S1) remain nearly unchanged after 50,000 cycles in the presence of HQBQ and HQ electrolytes. This is in contrast to the conventional polyaniline supercapacitor (P) where the internal resistance increases multiple times after long-term cycling due to the decomposition. When using BQ as the redox-active electrolyte, the charge transfer resistance is increased by a factor of ten after long cycling. This correlates well with the observed rapid decrease of the capacitance in the P-BQ device in Figure 2b.

The redox mechanism of quinones at single polyaniline-modified electrodes is well studied and is a complex process. Depending on the thickness of the polymer film, the quinone redox-processes can occur at the outer or inner phase of the porous polymer or between the polymer and the Pt surface.[17] In a simple picture, the redox mechanism in a polyaniline supercapacitor with two identical polymer-electrodes can be described as the following: the positive electrode is doped (oxidation of EM to PE) and the negative electrode is undoped (reducing EM to LE). In the discharged state of the supercapacitor (0 V) both electrodes are in the half oxidized/half reduced state (EM).[18] The detailed redox processes of the quinones are much more complex and are the subject of future studies. Potentially, both the reduction and oxidation of the mediating quinones can take place on both the positive and negative electrode.

Interestingly, only the mixtures containing HQ result in long-term cycling stability and stable capacitance of the supercapacitors. One plausible reason for the better performance of the HQ containing systems may be the enhanced solubility of HQ in aqueous systems. The rapid drop of capacitance in the P-BQ (without HQ) can be attributed to aggregation of BQ at the porous electrodes, inhibiting faradaic activity. The impedance data (Figure S1) confirm that the drop of capacitance in the conventional supercapacitor, P, is of different origin than that of the P-BQ supercapacitor. While both the internal- and charge-transfer resistance increase in the conventional device, P (decomposition of the polymer), only the charge-transfer resistance is increased in P-BQ after cycling. This suggests that the electronic properties of polyaniline in P-BQ are unchanged after long-term cycling. However, the detailed electrochemical mechanism needs to be further studied in detail.

Supercapacitors typically exhibit similar capacities over a broad range of discharge rates. The capacity depends on the mobility of the electrolytes and the thickness of the porous electrode network. In order to evaluate the interdependence of discharge rate, film thickness, and capacitance, galvanostatic experiments were performed using supercapacitors with polymer films of various thicknesses. The specific capacitance values increased in all supercapacitor devices in the presence of BQHQ electrolytes (Figure 2d). When thin polymer electrodes (~10 µm) were utilized, the C_s value increased by a factor of 5.5 compared to the pristine polymer devices (P) reaching a specific capacitance of 2646 F/g at the lowest measured current density (0.5 mA/cm^{-2}). In the case of the thicker polymer film (~67 µm), the C_s values in the P-BQHQ supercapacitor almost doubled (882 F/g). During discharge, a drop

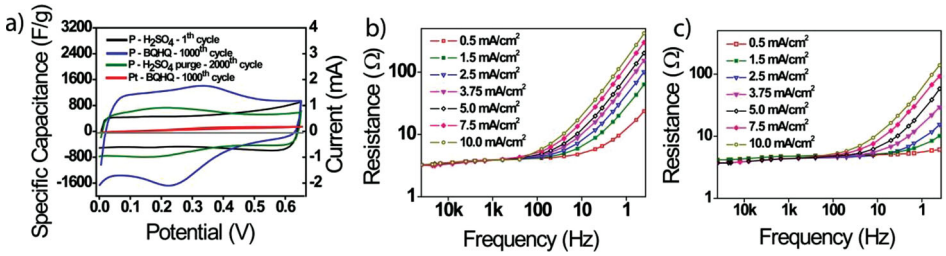

Figure 3. a) Cyclic voltammograms (25 mV/s) of the various supercapacitors (2-electrode configuration). Polyaniline supercapacitor P without quinones (black curve). P-BQHQ supercapacitor with BQHQ quinones (blue curve). P-BQHQ supercapacitor after removal of the quinones (green curve). CV of the supercapacitor with blank Pt-electrodes (red curve) and BQHQ (73 mM, 1:1) as redox-active electrolytes. b) Bode plot of the frequency *vs.* the resistance (at 10 mV) for the conventional supercapacitor P. c) Bode plot of the frequency *vs.* the resistance (at 10 mV) for the novel P-BQHQ supercapacitor. The supporting electrolyte in all supercapacitors was H_2SO_4 (1 M) with AcOH (30%).

of C_s was observed when the discharge rate exceeded a value of 2 mA/cm^2 (Figure 2d).

This point of transition is related to the transport of the BQHQ mediators. At low current rates more quinoid-molecules per unit time can flow through the porous films, enhancing the capacitance. This feature is absent in the case of the pristine polymer supercapacitors pointing to a different charge storage mechanism. Nevertheless, we note relatively high C_s values for the pristine polymer supercapacitor which is attributed to the sub-mm electrode films.

To understand at which electrochemical potential the redox-processes take place, the shape of the galvanostatic charge-discharge curves of the various supercapacitors were compared (Figure 2e). The conventional supercapacitor P in solely supporting electrolyte (Figure 2e, grey curve) exhibits a symmetric triangular-shaped charge-discharge curve which is typical for electrochemical supercapacitors.[3d,19] However, in the novel P-BQHQ supercapacitor (Figure 2e, black curve), the charge-discharge curve exhibits different slopes due to the addition of the mediating quinones. The steep slope of the discharge curve from P-BQHQ and short discharge time above 0.4 V points to a reduced charge storage capability at higher voltage. At lower potential (<0.4 V), the quinones and the polymer are both electrochemically active. The plateau below 100 mV points to additional quinone redox activity and is absent in the discharge curve of the P supercapacitor.

To evaluate the discharge behavior of supercapacitors without the polymer-surface (i.e. the redox behavior of the quinones at the Pt surface), galvanostatic cycling of Pt-BQHQ supercapacitors was performed. The inset in Figure 2d displays the charge-discharge curve (1 mA/cm^2) of a Pt-HQBQ device with no porous polyaniline films. The measured capacities are a few milifarads (Figure S2), which is three orders of magnitude lower than the capacities measured in polymer-devices and demonstrates that no significant capacitance can be generated at polymer-free Pt-electrodes. To compare the specific capacities of the Pt-electrodes and the porous polymer-modified electrodes, the areal capacities are displayed in Figure 2f. Negligible capacitance is measured for supercapacitors with Pt-electrodes and quinone electrolytes. When using polymer-modified electrodes and quinone electrolytes, the areal capacitance is increased at all discharge rates.

The increase in capacitance in the P-BQHQ supercapacitors is a result of a co-operative effect of the polymer-modified electrodes and the quinone electrolytes. Self-discharge is a well-known problem in supercapacitors and is particularly pronounced in polymeric supercapacitors.[3d] Depending on the thickness of the polymer films, we observe a loss of charge within minutes to one hour. This problem has to be addressed in the future and is related to the fast dissociation of the highly mobile quinone-electrolytes from the polymer modified-electrodes. However, it is demonstrated that the combination of the BQHQ and the polyaniline system results in stable supercapacitor devices with very high charge-capacity.

In order to determine if irreversible chemical reactions between polyaniline and the quinones occur, a series of long-term potentiostatic CV experiments on 2-electrode cells at 25 mV/s with the supercapacitors were conducted. The black CV curve in **Figure 3**a is the polyaniline supercapacitor P without quinones and it shows the characteristic box shape for electrochemical supercapacitors.[14,19] In the presence of the BQHQ electrolytes (Figure 3a, blue CV curve), additional redox features between 0.2 V and 0.4 V and near 0 V appeared which can be assigned to redox-processes of the quinones. The electrochemical activity of polyaniline is reduced at higher voltages during discharge as observed in the galvanostatic discharge experiments (Figure 2e). When the BQHQ electrolytes were removed, the original polymer behavior returns (Figure 3a, green CV curve). Therefore, most of the faradaic activity of the polyaniline is recovered after removal of the quinones. The weak redox signal at ~0.25 V can be attributed to the residual BQHQ in the system which could not be completely removed. As a control experiment we measure the CV (25 mV/s) of the polymer-free Pt-BQHQ (2-electrode) supercapacitor. The low measured current response Figure 3a (red curve) can be assigned to the oxidation of HQ to BQ. Moreover, the rapid decrease of the current during cycling as displayed in Figure S3 is due to the incomplete redox reaction and adsorption of the quinones on the blank platinum electrodes. This again demonstrates the great advantage of the polyaniline-modified electrodes to conduct reversible redox reactions in electrochemical supercapacitors.

The galvanostatic impedance technique allows analysis of the charge-transfer activity during device operation. To investigate the relationship between discharge rate and quinone redox-activity in the supercapacitors, we recorded individual in–situ single-frequency impedance-voltage curves (400 mHz-40 kHz). The obtained resistance values are plotted

Adv. Mater. **2014**,
DOI: 10.1002/adma.201400966

against the frequencies in Figure 3b/c at a constant voltage of 10 mV, where the quinone activity in the P-BQHQ devices is most pronounced. The resistance at high-frequencies (1 Hz to 40 kHz) corresponds to the electronic conductivity and is very comparable in both the conventional polymer supercapacitor P (Figure 3b) and the P-BQHQ supercapacitor (Figure 3c). However, the charge-transfer resistance at low frequencies (400 mHz-10 Hz) is different. In the conventional supercapacitor P with solely supporting electrolytes, the frequency/resistance relationship is independent of the discharge-rate (Figure 3b).

When HQBQ electrolytes are present a marked reduction of the resistance (400 mHz-10 Hz) is observed (Figure 3c) when the discharge current is slow (0.5 mA/cm^2). This points to the enhanced charge-transfer-processes of the quinones at the polymer-modified electrodes during slow discharge giving the high specific capacities.

In conclusion, we demonstrate a new approach for a stable polymer-supercapacitor. The polyaniline-benzoquinone supercapacitor gives simultaneously high pseudo-capacitance and unmatched cycling stability (>50,000). The increased capacitance in the polyaniline-quinone supercapacitor is attributed to the fast and reversible charge-transfer process between the polyaniline-modified electrodes and the quinones. Simultaneously, the extent of unfavorable redox processes in polyaniline is lowered – enhancing the long-term stability of the porous electrochemically active polymer. The combination of the quinone redox chemistry and acid-doped conductive polymer creates a low-pH supercapacitor device which is inherently stable.

Experimental Section

The polymeric supercapacitors were prepared as follows. The polymer electrodes were prepared by doping 20 mg of the commercially available polyaniline emeraldine-base (Sigma-Aldrich, average M_w ~50,000 g/mol) with H_2SO_4 (2.0 M, 200 µL) to form in-situ the emeraldine di-hydrogensulfate.[20] After addition of the acid, the blue color of the suspension (emeraldine-base) turned immediately to green (formation of the emeraldine salt). The green suspension was diluted with DMSO (200 µL) and sonicated for 45 min. The green polymer suspension was vigorously stirred each time before drop casting on mass-fabricated Pt-substrates (d = 200 nm, 1 cm^2) used as current collectors. The films were dried at 40 °C (1 h) and at room temperature (6 h) in the presence of air. No porous carbon material or other binder was used. The BQHQ (73 mM, 1:1) solution was freshly prepared by dissolving BQ and HQ in a solution of aqueous H_2SO_4 (1 M) with AcOH (30%) to dissolve the formed quinhydrone complex. The BQ (73 mM) and HQ (73 mM) solutions were prepared by dissolving the single quinone compound in H_2SO_4 (1 M) with AcOH (30%). The electrolyte solution was H_2SO_4 (1 M) with AcOH (30%) in all experiments where no quinones were used. The supercapacitor devices were fabricated by using two identical polymer electrodes. They were separated by a glass filter (~2 mm thick) soaked with electrolyte solution. Prior to long-cycling tests, the P-BQHQ and P-HQ supercapacitor devices were preconditioned by asymmetric galvanostatic charge-discharge cycles at constant current (2.5 mA/cm^2, 25 × ±0.65 V) in BQHQ electrolyte solution. Removal of the quinones in the cycled BQHQ-supercapacitors (Figure 3a) was conducted as the following. BQHQ-supercapacitors were soaked (2 h) in an aqueous solution of H_2SO_4 (0.5 M)/AcOH (15%)/MeOH (50%). The procedure was repeated three times to remove most of the quinones from the porous electrodes. All measured C_s values correspond to the point at steady state at maximum capacitance. The electrochemical cell behavior of the two-electrode supercapacitors and the 3-electrode cells were studied using a Bio-Logic VMP3 potentiostat. 3-electrode experiments were performed in a micro-cell with a Pt wire as counter electrode and Ag/AgCl (with sat. KCl, CH Instruments, USA, Part No. CHI111) as reference electrode.

Supporting Information

Supporting Information is available from the Wiley Online Library or from the author.

Acknowledgements

This work was supported by the Department of Energy Office of Basic Energy Sciences (DE-FG02–08ER46535) and by the Swiss National Science Foundation (SNF-PBBSP2–144291) and the battery fabrication and testing lab, part of the MRL Shared Experimental Facilities, supported by the MRSEC Program of the NSF under Award No. DMR 1121053; a member of the NSF-funded Materials Research Facilities Network. Fellowship support to KAS from the ConvEne IGERT Program of the National Science Foundation (DGE 0801627), and support from the *Fred and Linda R. Wudl Chair* is gratefully acknowledged.

Received: March 1, 2014
Revised: May 9, 2014
Published online:

[1] a) R. Kötz, M. Carlen, *Electrochim. Acta* **2000**, *45*, 2483–2498; b) J. R. Miller, P. Simon, *Science* **2008**, *321*, 651–652; c) H. Li, Q. Zhao, W. Wang, H. Dong, D. Xu, G. Zou, H. Duan, D. Yu, *Nano Lett.* **2013**, *13*, 1271–1277.
[2] L. L. Zhang, X. S. Zhao, *Chem. Soc. Rev.* **2009**, *38*, 2520–2531.
[3] a) S. Roldán, C. Blanco, M. Granda, R. Menéndez, R. Santamaría, *Angew. Chem. Int. Ed.* **2011**, *50*, 1699–1701; b) P. Simon, Y. Gogotsi, *Nat. Mater.* **2008**, *7*, 845–854; c) G. A. Snook, P. Kao, A. S. Best, *J. Power Sources* **2011**, *196*, 1–12; d) G. Wang, L. Zhang, J. Zhang, *Chem. Soc. Rev.* **2012**, *41*, 797–828.
[4] G. Milczarek, O. Inganäs, *Science* **2012**, *335*, 1468–1471.
[5] a) Y. Meng, K. Wang, Y. Zhang, Z. Wei, *Adv. Mater.* **2013**, *25*, 6985–6990; b) S. Roldán, M. Granda, R. Menéndez, R. Santamaría, C. Blanco, *J. Phys. Chem. C* **2011**, *115*, 17606–17611; c) S. Roldán, M. Granda, R. Menéndez, R. Santamaría, C. Blanco, *Electrochim. Acta* **2012**, *83*, 241–246; d) H. Yu, J. Wu, L. Fan, Y. Lin, K. Xu, Z. Tang, C. Cheng, S. Tang, J. Lin, M. Huang, Z. Lan, *J. Pow. Sources* **2012**, *198*, 402–407.
[6] C. Peng, D. Hu, G. Z. Chen, *Chem. Comm.* **2011**, *47*, 4105–4107.
[7] a) A. J. Heeger, *Angew. Chem. Int. Ed.* **2001**, *40*, 2591–2611; b) A. J. Heeger, *Semiconducting and metallic polymers*, Oxford University Press, Oxford, New York **2010**.
[8] J. Huang, R. B. Kaner, *J. Am. Chem. Soc.* **2004**, *126*, 851–855.
[9] a) H. Lin, L. Li, J. Ren, Z. Cai, L. Qiu, Z. Yang, H. Peng, *Sci. Rep.* **2013**, *3*; 1353 b) L. Yuan, X. Xiao, T. Ding, J. Zhong, X. Zhang, Y. Shen, B. Hu, Y. Huang, J. Zhou, Z. L. Wang, *Angew. Chem. Int. Ed.* **2012**, *51*, 4934–4938; c) Q. Wu, Y. Xu, Z. Yao, A. Liu, G. Shi, *ACS Nano* **2010**, *4*, 1963–1970; d) C. Meng, C. Liu, L. Chen, C. Hu, S. Fan, *Nano Lett.* **2010**, *10*, 4025–4031.
[10] L. Nyholm, G. Nyström, A. Mihranyan, M. Strømme, *Adv. Mater.* **2011**, *23*, 3751–3769.
[11] A. Burke, *Electrochim. Acta* **2007**, *53*, 1083–1091.
[12] A. G. MacDiarmid, *Angew. Chem. Int. Ed.* **2001**, *40*, 2581–2590.
[13] R. E. Moser, H. G. Cassidy, *J. Am. Chem. Soc.* **1965**, *87*, 3463–3467.

[14] M. D. Stoller, R. S. Ruoff, *Energy Environ. Sci.* **2010**, *3*, 1294–1301.
[15] a) E. Smela, W. Lu, B. R. Mattes, *Synth. Metals* **2005**, *151*, 25–42; b) A. A. Pud, *Synth. Metals* **1994**, *66*, 1–18.
[16] W. Takashima, M. Fukui, M. Kaneko, K. Kaneto, *Jap. J. Appl. Phys.*, *34*, 3786–3789.
[17] a) A. Malinauskas, R. Holze, *Electrochim. Acta* **1998**, *43*, 2563–2575; b) J. C. Cooper, E. A. H. Hall, *Electroanalysis* **1993**, *5*, 385–397; c) Z. Mandi , L. Dui , *J. Electroanal. Chem.* **1996**, *403*, 133–141.
[18] A. Rudge, J. Davey, I. Raistrick, S. Gottesfeld, J. P. Ferraris, *J. Power Sources* **1994**, *47*, 89–107.
[19] V. Khomenko, E. Frackowiak, F. Béguin, *Electrochim. Acta* **2005**, *50*, 2499–2506.
[20] W.-S. Huang, B. D. Humphrey, A. G. MacDiarmid, *J. Chem. Soc., Faraday Trans. 1* **1986**, *82*, 2385–2400.

Adv. Mater. **2014**,
DOI: 10.1002/adma.201400966